Small core FBG-based temperature compensated 'smart' contact lens for effective intraocular pressure measurement

Ye Chen [a,*], Jun Wang [b], Yin Zhao [c], Xiao-Jun Liu [b], Hong Zhang [c], Ian Murdoch [d], Chris Hull [e], John Barbur [e], Tong Sun [a,**], KennethT.V. Grattan [a]

[a] *Department of Electrical & Electronic Engineering, School of Mathematics, Computer Science & Engineering, City, University of London, Northampton Square, London, EC1V 0HB, United Kingdom*
[b] *State Key Laboratory of Digital Manufacturing Equipment and Technology, School of Mechanical Science and Engineering, Huazhong University of Science and Technology, Wuhan, 430074, PR China*
[c] *Department of Ophthalmology, Tongji Hospital, Tongji Medical College, Huazhong University of Science and Technology, Wuhan, 430030, PR China*
[d] *Institute of Ophthalmology, University College London, Bath Street, EC1V 9EL, London, United Kingdom*
[e] *Centre for Applied Vision Research, School of Health Sciences, City, University of London, London, EC1R 1UB, United Kingdom*

ARTICLE INFO

ABSTRACT

In this work, a small core, Fibre Bragg Grating (FBG)-based smart contact lens for intraocular pressure (IOP) measurement has been demonstrated. Further, an integral temperature compensation mechanism has been developed and included in the sensor design, allowing it to offer good long-term measurement capability while allowing for any local temperature fluctuations. The sensitivity of the device has been shown to be 12.9 p.m./mmHg, yielding good repeatability in tests carried out. Such a small core fibre, FBG-based smart contact lens shows significant potential for improving the management and therapy of glaucoma, the second most common cause of preventable blindness in the world.

1. Introduction

Glaucoma is one of the world's leading causes of blindness [1]. It is described as a group of eye diseases that lead to damage of the optic nerve (optic neuropathy) and vision loss. A major risk factor for glaucoma is increased intraocular pressure (IOP). Although vision that has been lost due to glaucoma is irreversible, with early diagnosis, careful monitoring and appropriate treatment such as therapy, further vision loss can be prevented or reduced. With therapy, most patients retain useful sight for life [2]. Since glaucoma has been described as the 'silent thief of sight' because it progresses slowly and there are few noticeable warning signs, initiatives to increase public awareness and make comprehensive eye examinations easier are the key to reducing or eliminating undiagnosed glaucoma. This can be supported through regular IOP monitoring which is critical to help manage the disease [3]. (see Table 1)

Lowering of IOP is the principal therapy available for the management of glaucomas [4]. Current IOP measurements are generally done during a visit to the clinician's office or surgery. In a similar fashion to blood-pressure monitoring, a one-time measurement does not represent the overall risk. The IOP also shows diurnal variation which is greater in diseased eyes [5] and these fluctuations have been shown to be associated with glaucoma progression [6,7]. The most usual method of tonometry is the current 'gold standard' Goldmann applanation. For logistical reasons, phasing (measurement of the IOP throughout the day) is generally limited to being done within office hours, which means the peaks and troughs may be missed if they occur outside these working hours [8,9]. However, the benefit of continuous, simple IOP measurement not requiring an independent observer to be present, is clear.

Researchers previously have developed methods for continuous IOP monitoring by using implanted pressure sensors, MEMs chips and eye curvature monitoring [10–17]. Pressure sensor implants require surgery and the devices consume high wireless power during their operation, thereby reducing patient compliance and causing problems due to device temperature rises. The on-lens eye curvature method is less invasive and can provide direct access to the eye surface with minimal disturbances. However, the electronic, contact lens-based devices used to monitor such changes cannot work in situations where there is strong electromagnetic interference, such as when various scans are being undertaken. Thus,

Table 1
Measurement metrics of the presented IOP sensor.

Sensitivity	12.9 ± 0.2 p.m./mmHg
Measurement range	0–30 mmHg
Uncertainty	±0.1 mmHg

there is a demand for new methods which will allow measurements to be taken when there is significant electromagnetic interference present e.g. with high levels of wireless power or X-rays or MRI and the approach is to develop a sensor within the contact lens that can communicate IOP readings without extra aerials, battery packs or recorders. As a consequence, a new fibre optic-based technique that eliminates such problems is discussed and its performance evaluated.

In recent years, optical fibre-based wearable sensors [18–27] have been developing very rapidly due to their important properties of high sensitivity, thin fibre (sensor) diameter and thus ease of bending the fibre to fit the body and simplicity of integration of the sensor with the person. The ability of optical fibre sensors to operate even with high levels of electromagnetic interference make them suitable to work in situations where such interference is present and allow verifiable measurements to be made. Contact lenses, which are long established with low rates of complications if handled correctly, can provide a suitable host for such a sensor, as has previously been demonstrated. However, incorporating an optical fibre into such a lens and making it comfortable is a challenge and commercial single mode optical fibres (of typical diameter 125 μm, equivalent to a human hair and used widely in telecommunications applications) could lead to discomfort issue in normal use. In addition, the rigidity of fibre could cause contact lens deformation and reduce the quality of the fit and change the refractive power of the lens as a result. In this work, this particular problem could be reduced with the integration of a smaller core optical fibre into a commercial contact lens, minimizing discomfort to the wearer.

The aim of this study thus has been to develop an innovative optical fibre sensor using a small diameter optical fibre integrated into a temperature-compensated smart contact lens with the fibre containing a Fibre Bragg Grating (FBG) designed to allow continuous IOP measurement. The theoretical background to the research is discussed and the experimental arrangement used is described, with results from tests carried out reported and conclusions on the outcomes of the study drawn.

2. Theoretical background

Previous studies of intraocular pressure effects have shown that the IOP changes will cause different corneal thickness variations [28]. The approach used here has been to create a FBG-integrated contact lens to measure changes in corneal curvature transmitted from the anterior corneal surface/tearfilm to the contact lens developed where the curvature change stretches the FBG, altering the grating spacing and thereby causing a wavelength shift. Thus the contact lens system used in this

work was designed around a two FBG-based sensor, with integrated temperature compensation.

A schematic of the device is shown in Fig. 1(a), illustrating the design of the system to achieve the small core FBG based smart contact lens sensor. In this design, two small core in-fibre Bragg gratings (FBGs) are located as shown, at different distances from the centre of the contact lens. Fig. 1(b) shows a photograph of the actual sensor showing the fabricated sensor using the contact lens with the small core FBG attached. The contact lens used was a commercial lens of diameter 14 mm and thickness 90 μm (PureVision made by Bausch & Lomb). The diameter of the small core fibre is 50 μm. The length of the FBGs written into the fibre was 5 mm. The wavelengths of the two FBGs are 1545 nm and 1569 nm, respectively. One of the FBGs was located in the centre of the contact lens and the other was mounted close to the edge of the lens as designed.

Previous work [28] has suggested that the IOP change will cause a larger deformation in centre region of the eyeball, compared to that seen at the edge. Thus the FBG located close to centre will show the larger wavelength shift. Any temperature variations, however, will cause similar wavelength shifts to both the FBGs used in the sensor. Based on these properties, the effects of the temperature and IOP changes can be represented by:

$$\begin{cases} \Delta\lambda_1 = S_{T1} \cdot \Delta T + S_{IOP1} \cdot \Delta P_{IOP} \\ \Delta\lambda_2 = S_{T2} \cdot \Delta T + S_{IOP2} \cdot \Delta P_{IOP} \end{cases} \tag{1}$$

where $\Delta\lambda_1$ and $\Delta\lambda_2$ are the wavelength shifts associated with FBG1 and FBG2 when subjected to pressure (IOP) and temperature variations; S_{T1} and S_{T2} are the temperature sensitivities of FBG1 and FBG2; S_{IOP1} and S_{IOP2} are the sensitivities to IOP of both FBGs. ΔT and ΔP_{IOP} are temperature and IOP changes, respectively that occur during the experiment.

From these equations, the IOP change can then be calculated from:

$$\Delta P_{IOP} = \frac{\Delta\lambda_2 - C_T \Delta\lambda_1}{S_{IOP2} - C_T S_{IOP1}} \tag{2}$$

where here, $C_T = S_{T2}/S_{T1}$ is the temperature compensation coefficient of the FBGs used.

3. Experimental arrangement

The fabrication of the 'smart' contact lens can be divided into following steps: (1) small core fibre into which two FBGs were fabricated at known (and similar) wavelengths using a UV laser and appropriate phase masks was selected where the length of the FBGs used are, as discussed, ∼5 mm. The wavelengths chosen for the two FBGs written into the fibre are 1545 nm and 1569 nm, respectively; (2) the fibre surface was cleaned and functioned with polymerizable groups so that it can adhere evenly to the contact lens; (3) the fibre was bent to form a spiral line– this being facilitated by the small core fibre used –to follow the curved shape of the lens using tweezers. The fibre was then stuck onto the
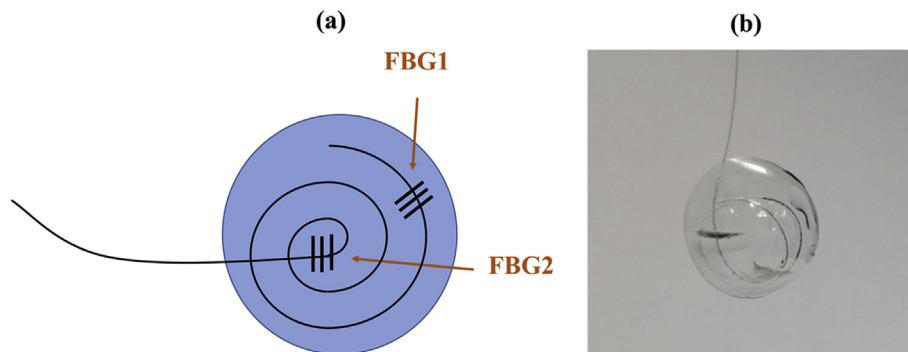
Fig. 1. (a) The design of the small core FBG-based contact lens; (b) a photograph of the smart contact lens that has been fabricated in this work.

surface of the selected contact lens, using the commercial cyanoacrylic adhesive. Loctite 4850 glue was used here as it gives instant adhesion and it is flexible – characteristics that are ideal for this application. This fibre spiral fitted well the contact lens used (which was of diameter 14 mm and thickness 90 μm). One of the FBGs was located in the centre of the contact lens (primarily to measure the IOP) and the other was mounted close to the edge of the lens (to monitor the temperature); (4) the sensor thus produced was then cured in air and quickly placed in commercial contact lens storage liquid.

To calibrate the temperature compensation coefficient, the following process was undertaken. The temperature of the storage liquid (and thus of the lens) was increased, following which the contact lens was allowed to cool to room temperature. Fig. 2 (a) shows the responses of the two FBGs used to this temperature change – the results show that they have closely matched temperature sensitivities, which agrees well with the theoretical analysis set out earlier. From Fig. 2 (b), the linear fitted temperature compensation coefficient monitored was 1.24 ± 0.02. It is noted that the temperature of a contact lens on a living eye will be typically ~34 °C and thus small variations in and around that temperature can be measured with this system.

Fig. 3 shows the experimental setup used in the measurement of the IOP change. To do so, a needle is inserted into an excised pig eye from the back of the eyeball [29]. The IOP inside the excised eye was changed using a simple manometer using a reservoir containing water where the variation in the height of the reservoir enabled the pressure to be varied. A PVC syringe tube from the reservoir was connected to the needle and a pressure gauge (to act as a reference), using a 3-channel connector. The optical fibre was connected to a FBG interrogator (sm125 type, Micron Optics) to allow a continuous measurement to be made (where the resolution of the interrogator is 1 p.m. and the sampling rate is 2 Hz).

In this work a pig's eye was used as a proxy for the human eye – the pig eye is an *ex vivo* animal model often used in vision sciences research because its morphology is similar to the human eye [19]. The smart contact lens was carefully placed on the pig eye and any bubbles removed to create a good contact between the eye and the contact lens. The pig eye was located in a shallow dish filled with water to keep it moist during the experiment. A syringe needle was then moved from side of the eye, into the anterior chamber of the eye, to create the variation in the IOP of the eye, where the syringe was connected to a small bottle of water hanging overhead, allowing the hydraulic pressure to change in the eyeball, causing its IOP to increase or decrease in a reproducible way. The pressure change can be calibrated by use of the pressure gauge shown in Fig. 3, controlling the IOP change step size to be ~2 mmHg.

Fig. 4 (a) illustrates the wavelength shifts of the FBGs built into the contact lens with time, when IOP increase from 5 to 25 mmHg (and with this reversed for Fig. 4 (b)). These figures show that the wavelength associated with FBG2, which is located in the centre of the lens (as shown in Fig. 1 (a)), is red-shifted when the IOP increases (and conversely blueshifts when the IOP decreases). By contrast, the grating FBG1 on the
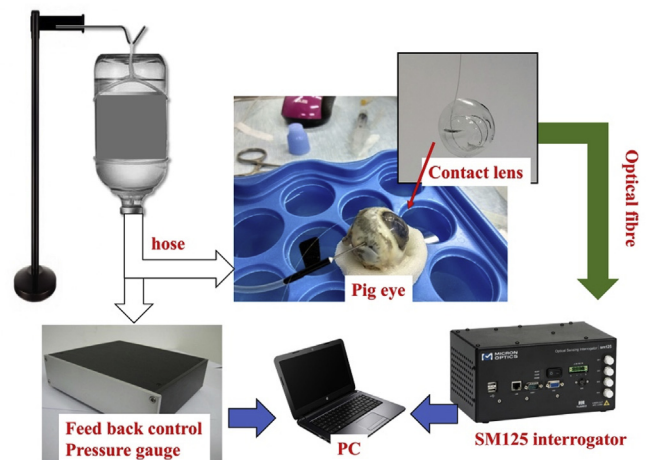

Fig. 3. Schematic of the experiment setup used in this work.

edge of the contact lens (see Fig. 1 (a)) shows a very small wavelength shift in both cases, likely due to the circumferential rather than radial orientation of the FBG sensor, as would be expected from the discussion above.

The data from Fig. 4 is then used to create Fig. 5, which illustrates the (essentially linear) fit of FBG2 wavelength shift with IOP change. Here the pressure sensitivity, measured using FBG2 is shown to be 12.9 ± 0.2 p.m./mmHg, contrasting with the sensitivity of FBG1 which is only ~0.5 p.m./mmHg, some 25 times less than that of FBG2. This enables FBG2 to be used for pressure (and temperature) measurement and within experimental error for FBG1 to be used to provide a correction for any temperature changes during the experiment. This dual FBG-based set up allows for effective temperature compensation to be applied, although many *in vivo* studies will be undertaken at a stable body temperature.

The dynamic response of the sensor system is good, in that the increase and subsequent decrease in the pressure provides responses from the sensor which show good repeatability. The normal range for human intraocular pressure is known to be within the range 10 mmHg–21 mmHg, this being done to maintain the normal shape of the eyeball. Measurement accuracy can be improved by using the temperature compensation which is 'built-in' to the measurement method and through a longer time averaging of the signal from the FBGs which comprise the sensor, as the pressure signal will not normally change on a second by second basis. Diurnal variation monitoring is important, as it is greater in diseased eyes [5], and the sensor system developed here (with integrated temperature compensation) is relatively easy to wear, thus providing an accurate measurement method for periods of up to 24 h in continuous monitoring, to support early glaucoma diagnosis.

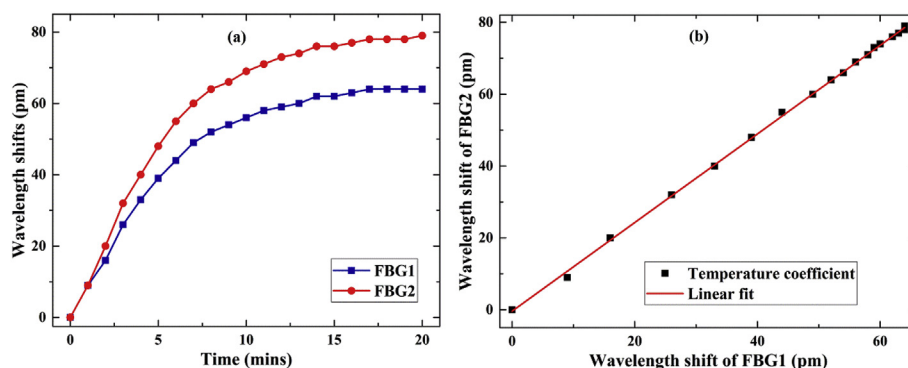In this study, while temperature compensation was available from the

Fig. 2. (a) Wavelength shift response of two FBGs with temperature decrease. (b) Linear fit of the temperature compensation grating, FBG1, showing the temperature coefficient.
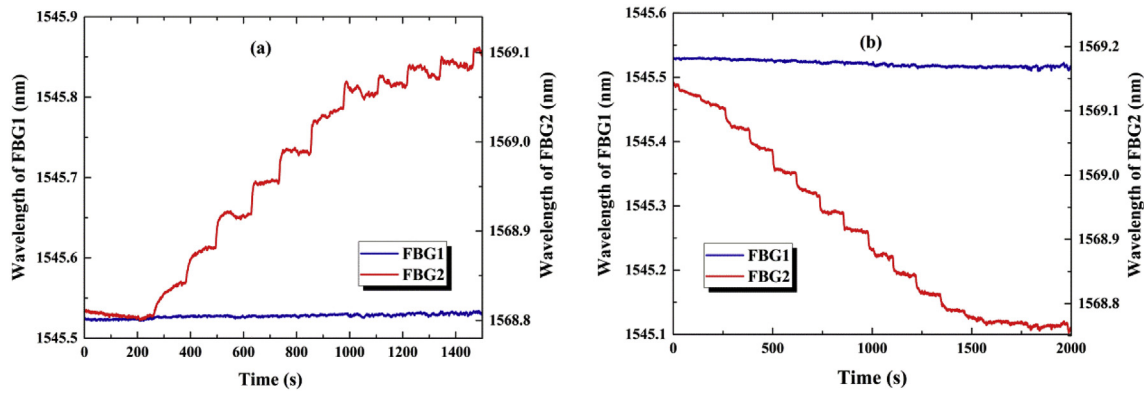
Fig. 4. (a) Wavelength shift of two FBGs with IOP increases; (b) wavelength shifts when IOP decreases.
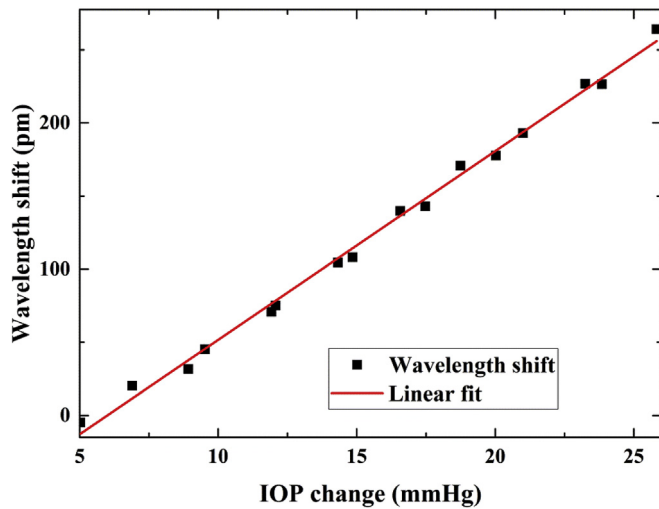

Fig. 5. Graph of FBG2 wavelength shifts with IOP variation over the range from 5 mmHg to 27 mmHg (the linear fitted sensitivity – the slope of the graph – is 12.9 ± 0.2 p.m./mmHg).

use of the second FBG, there was no need to apply it due to the stable operating conditions of the experiment carried out. However, this may not always be the case and thus it was seen as important to have the facility for integral temperature compensation which could be provided using the data in Fig. 2 (b).

4. Conclusion

In this work, a 'smart' contact lens sensor system has been developed, based on the use of a small core optical fibre into which FBGs have been written (including one to provide temperature compensation, as needed). The sensor uses a small fibre diameter (of 50 μm) which can readily be bent and thus easily integrated into a commercial contact lens. The smart contact lens sensing system developed has two FBGs integrated into the fibre, to allow temperature compensation of the sensor.

The work done to evaluate the performance of the device shows that the 'smart' contact lens sensor thus developed has a sensitivity about 12.9 ± 0.2 p.m./mmHg when used to measure intraocular pressure in a test carried out. The sensor has additional functionality in that temperature influences could be compensated as needed to allow the sensor to show real potential for continuous IOP measurement in a patient, even when subjected to strong electromagnetic interference from exposure to such sources during other hospital assessments. Thanks to the advantages of easy integration of multiple FBGs with optical fibre, increasing the number of FBGs to fully measure the intraocular pressure distribution is possible. Given the sensitivity of the device, in light of the range of IOP which is symptomatic of glaucoma, it shows significant potential for continuous IOP measurement in human eyes and thus to aid glaucoma management and therapy.

Conflict of interest statement

We declare that we have no financial and personal relationships with other people or organizations that can inappropriately influence our work, there is no professional or other personal interest of any nature or kind in any product, service and/or company that could be construed as influencing the position presented in, or the review of, the manuscript entitled "Small core FBG-based 'smart' contact lens for intraocular pressure measurement".

Acknowledgements

References

[1] H.A. Quigley, A.T. Broman, The number of people with glaucoma worldwide in 2010 and 2020, Br. J. Ophthalmol. 90 (2006) 262–267, https://doi.org/10.1136/bjo.2005.081224.

[2] Glaucoma: diagnosis and management, n.d. https://www.nice.org.uk/guidance/ng81. (Accessed 20 March 2019).

[3] Glaucoma, Moorfields eye charity. https://moorfieldseyecharity.org.uk/glaucoma, 2018. (Accessed 15 March 2019).

[4] A.L. Coleman, S. Miglior, Risk factors for glaucoma onset and progression, Surv. Ophthalmol. 53 (2008) S3–S10, https://doi.org/10.1016/j.survophthal.2008.08.006.

[5] J.H.K. Liu, X. Zhang, D.F. Kripke, R.N. Weinreb, Twenty-four-Hour intraocular pressure pattern associated with early glaucomatous changes, Investig. Ophthalmol. Vis. Sci. 44 (2003) 1586–1590, https://doi.org/10.1167/iovs.02-0666.

[6] M.O. Gordon, J.A. Beiser, J.D. Brandt, D.K. Heuer, E.J. Higginbotham, C.A. Johnson, J.L. Keltner, J.P. Miller, R.K. Parrish, M.R. Wilson, M.A. Kass, The Ocular Hypertension Treatment Study: baseline factors that predict the onset of primary open-angle glaucoma, Arch. Ophthalmol. Chic. Ill 1960 120 (2002) 714–720, discussion 829-830.

[7] B. Bengtsson, M.C. Leske, L. Hyman, A. Heijl, Fluctuation of intraocular pressure and glaucoma progression in the early manifest glaucoma trial, Ophthalmology 114 (2007) 205–209, https://doi.org/10.1016/j.ophtha.2006.07.060.

[8] J.H.K. Liu, D.F. Kripke, M.D. Twa, R.E. Hoffman, S.L. Mansberger, K.M. Rex, C.A. Girkin, R.N. Weinreb, Twenty-Four–hour pattern of intraocular pressure in the aging population, Investig. Ophthalmol. Vis. Sci. 40 (1999) 2912–2917.

[9] J.T. Wilensky, D.K. Gieser, M.L. Dietsche, M.T. Mori, R. Zeimer, Individual variability in the diurnal intraocular pressure curve, Ophthalmology 100 (1993) 940–944, https://doi.org/10.1016/S0161-6420(93)31551-4.

[10] E.Y. Chow, A.L. Chlebowski, P.P. Irazoqui, A miniature-implantable Rf-wireless active glaucoma intraocular pressure monitor, IEEE Trans. Biomed. Circuits Syst. 4 (2010) 340–349, https://doi.org/10.1109/tbcas.2010.2081364.

[11] G. Chen, H. Ghaed, R. Haque, M. Wieckowski, Y. Kim, G. Kim, D. Fick, D. Kim, M. Seok, K. Wise, D. Blaauw, D. Sylvester, A cubic-millimeter energy-autonomous wireless intraocular pressure monitor, in: 2011 IEEE Int. Solid-State Circuits Conf, 2011, https://doi.org/10.1109/isscc.2011.5746332 nil.

[12] A. Donida, G.D. Dato, P. Cunzolo, M. Sala, F. Piffaretti, P. Orsatti, D. Barrettino, A circadian and cardiac intraocular pressure sensor for smart implantable lens, IEEE Trans. Biomed. Circuits Syst. nil (2016), https://doi.org/10.1109/tbcas.2015.2501320, 1–1.

[13] N.M. Farandos, A.K. Yetisen, M.J. Monteiro, C.R. Lowe, S.H. Yun, Contact lens sensors in ocular diagnostics, Adv. Healthc. Mater. 4 (2014) 792–810, https://doi.org/10.1002/adhm.201400504.

[14] C. Faschinger, G. Mossböck, Continuous 24 h monitoring of changes in intraocular pressure with the wireless contact lens sensor Triggerfish™. First results in patients, Ophthalmol. Z. Dtsch. Ophthalmol. Ges. 107 (2010) 918–922, https://doi.org/10.1007/s00347-010-2198-4.

[15] M. Leonardi, E.M. Pitchon, A. Bertsch, P. Renaud, A. Mermoud, Wireless contact lens sensor for intraocular pressure monitoring: assessment on enucleated pig eyes, Acta Ophthalmol. 87 (2009) 433–437, https://doi.org/10.1111/j.1755-3768.2008.01404.x.

[16] J. Kim, M. Kim, M.-S. Lee, K. Kim, S. Ji, Y.-T. Kim, J. Park, K. Na, K.-H. Bae, H.K. Kim, F. Bien, C.Y. Lee, J.-U. Park, Wearable smart sensor systems integrated on soft contact lenses for wireless ocular diagnostics, Nat. Commun. 8 (2017) 14997, https://doi.org/10.1038/ncomms14997.

[17] J.-C. Chiou, S.-H. Hsu, Y.-C. Huang, G.-T. Yeh, W.-T. Liou, C.-K. Kuei, A wirelessly powered smart contact lens with reconfigurable wide range and tunable sensitivity sensor readout circuitry, Sensors 17 (2017) 108, https://doi.org/10.3390/s17010108.

[18] B.M. Quandt, L.J. Scherer, L.F. Boesel, M. Wolf, G.-L. Bona, R.M. Rossi, Body-monitoring and health supervision by means of optical fiber-based sensing systems in medical textiles, Adv. Healthc. Mater. 4 (2014) 330–355, https://doi.org/10.1002/adhm.201400463.

[19] K. Peters, Polymer optical fiber sensors-A review, Smart Mater. Struct. 20 (2010), https://doi.org/10.1088/0964-1726/20/1/013002, 013002.

[20] C. Díaz, C. Leitão, C. Marques, M. Domingues, N. Alberto, M. Pontes, A. Frizera, M. Ribeiro, P. André, P. Antunes, Low-cost interrogation technique for dynamic measurements with fbg-based devices, Sensors 17 (2017) 2414, https://doi.org/10.3390/s17102414.

[21] H. Li, H. Yang, E. Li, Z. Liu, K. Wei, Wearable sensors in intelligent clothing for measuring human body temperature based on optical fiber Bragg grating, Opt. Express 20 (2012) 11740, https://doi.org/10.1364/oe.20.011740.

[22] L. Dziuda, J. Lewandowski, F. Skibniewski, G. Nowicki, Fibre-optic sensor for respiration and heart rate monitoring in the mri environment, Procedia Eng 47 (2012) 1291–1294, https://doi.org/10.1016/j.proeng.2012.09.391.

[23] M. Krehel, M. Schmid, R. Rossi, L. Boesel, G.-L. Bona, L. Scherer, An optical fibre-based sensor for respiratory monitoring, Sensors 14 (2014) 13088–13101, https://doi.org/10.3390/s140713088.

[24] C. Massaroni, A. Nicolò, D.L. Presti, M. Sacchetti, S. Silvestri, E. Schena, Contact-based methods for measuring respiratory rate, Sensors 19 (2019) 908, https://doi.org/10.3390/s19040908.

[25] A.G. Leal-Junior, C.R. Díaz, C. Leitão, M.J. Pontes, C. Marques, A. Frizera, Polymer optical fiber-based sensor for simultaneous measurement of breath and heart rate under dynamic movements, Opt. Laser. Technol. 109 (2019) 429–436, https://doi.org/10.1016/j.optlastec.2018.08.036.

[26] J. Nedoma, M. Fajkus, R. Martinek, Fiber-optic breath sensors: a comparison study, J. Biomim. Biomater. Biomed. Eng. 40 (2019) 56–63, https://doi.org/10.4028/www.scientific.net/jbbbe.40.56.

[27] A. Aitkulov, D. Tosi, Optical fiber sensor based on plastic optical fiber and smartphone for measurement of the breathing rate, IEEE Sens. J. nil (2019), https://doi.org/10.1109/jsen.2019.2894834, 1–1.

[28] A. Elsheikh, C.W. McMonnies, C. Whitford, G.C. Boneham, In vivo study of corneal responses to increased intraocular pressure loading, Eye Vis 2 (2015) 20, https://doi.org/10.1186/s40662-015-0029-z.

[29] I. Sanchez, R. Martin, F. Ussa, I. Fernandez-Bueno, The parameters of the porcine eyeball, Graefes Arch. Clin. Exp. Ophthalmol. 249 (2011) 475–482, https://doi.org/10.1007/s00417-011-1617-9.